Eur. Phys. J. B **28**, 415–422 (2002)
DOI: 10.1140/epjb/e2002-00245-3

THE EUROPEAN PHYSICAL JOURNAL B

Mechanism of grain-boundary magnetoresistance in Fe_3O_4 films

M. Ziese[a], R. Höhne, H.C. Semmelhack, H. Reckentin, N.H. Hong, and P. Esquinazi

Department of Superconductivity and Magnetism, University of Leipzig, Linnéstrasse 5, 04103 Leipzig, Germany

Received 15 April 2002
Published online 13 August 2002 –

Abstract. The magnetotransport properties of magnetite films with different microstructures were investigated in order to identify prerequisites for the attainment of a large tunnelling magnetoresistance in polycrystalline samples. Epitaxial films on $MgAl_2O_4$, polycrystalline films on Al_2O_3 and rough $MgAl_2O_4$ substrates and a polycrystalline $La_{0.7}Ca_{0.3}MnO_3$ film on MgO were compared. Although grain boundaries induce a large high-field magnetoresistance in magnetite films, the low-field magnetoresistance characteristic for spin-polarized tunnelling was virtually absent in these samples. Two factors might be responsible for this behaviour: (1) grain boundaries in magnetite are conducting and do not form tunnelling barriers and (2) the spin-polarization near grain boundaries is suppressed due to non-stoichiometry.

PACS. 72.25.-b Spin polarized transport – 73.50.Jt Galvanomagnetic and other magnetotransport effects (including thermomagnetic effects) – 75.70.-i Magnetic properties of thin films, surfaces, and interfaces

1 Introduction

In recent years extrinsic magnetoresistance phenomena in magnetic oxides have been intensively studied [1]. Extrinsic magnetoresistance arises from spin-dependent scattering at extended defects or from spin-polarized tunnelling; it has been investigated in a variety of materials such as the colossal magnetoresistance (CMR) manganites [2,3], CrO_2 [4], $Tl_2Mn_2O_7$ [5], the double perovskite Sr_2FeMoO_6 [6] as well as magnetite. These studies were performed in the hope to optimize devices based on magnetic oxides in planar structure in order to find a magnetoresistance signal at room temperature that would make oxides competitive with giant magnetoresistance (GMR) multilayers. Up to now these attempts have largely failed for a number of reasons [1]; the most important of these is the low Curie temperature of ferromagnetic oxides that makes these materials useless for operation in the range between room temperature and 500 K.

There is one exception: the ferrimagnet magnetite (Fe_3O_4) with a Curie temperature of 858 K. Magnetite has an exceptionally high conductivity among the ferrites due to the mixed valence character of Fe^{2+}/Fe^{3+} ions occupying the octahedral B-sites of the spinel lattice. Moreover, band-structure calculations indicate that magnetite is a half-metal with only minority carriers at the Fermi level [7]; accordingly, the spin-polarization is $P = -1$. The half-metallic nature, however, is still under discussion, see Srinitiwarawong and Gehring [8]. There have been numerous attempts to fabricate polycrystalline magnetite samples with high grain-boundary magnetoresistance [9–16] or tunnelling junctions with magnetite electrodes [17,18]. These were unsuccessful with magnetoresistance values of only a few percent in applied fields of the order of one Tesla. A breakthrough came recently with studies along two different routes. Versluijs *et al.* [19,20] investigated the magnetoresistance of nanocontacts between Fe_3O_4 crystals. The nanocontacts exhibit nonlinear current-voltage curves as well as magnetoresistance ratios up to 85%. This was interpreted as arising from domain-wall scattering within a model of a magnetic balloon effect. On the other hand, Chen *et al.* [21] found a large magnetoresistance at room temperature in polycrystalline $Zn_{0.41}Fe_{2.59}O_4$. This was an astonishing result, since the Curie temperature is only 318 K. The magnetoresistance seems to arise from spin-polarized tunnelling through insulating α-Fe_2O_3 barriers surrounding the $Zn_{0.41}Fe_{2.59}O_4$ grains; the authors speculated on a mainly antiferromagnetic coupling of zinc ferrite grains mediated by the haematite spacer layers.

In this work we compare magnetoresistance data on epitaxial and polycrystalline magnetite films. The issue we want to address is the identification of the necessary prerequisites for a large grain-boundary magnetoresistance in magnetite films. The data indicate that two factors are vital: on the one hand stoichiometry near the grain boundary must be controlled in order to obtain a high spin-polarization, on the other hand intergrain magnetic coupling across the grain boundary must be sufficiently weak to facilitate abrupt magnetization changes.

2 Experimental details

Magnetite films were grown on $MgAl_2O_4(001)$ and sapphire $(Al_2O_3)(0001)$ substrates by pulsed laser deposition from a stoichiometric, polycrystalline magnetite

[a] e-mail: ziese@physik.uni-leipzig.de

target [22]. Deposition temperature was 580 °C and oxygen partial pressure to achieve optimal magnetic and transport properties was 5×10^{-6} mbar. A Lambda-Physik Excimer laser at a wavelength of 248 nm (KrF) operated at a repetition rate of 10 Hz and a pulse energy of 0.6 J was used; the fluence was about 2.5 J/cm^2. In this work data on four magnetite films are presented: (1) an epitaxial film produced on an epi-polished $MgAl_2O_4$ substrate, (2) a polycrystalline film on epi-polished sapphire as well as (3) and (4) polycrystalline films produced on the rough backside of $MgAl_2O_4$ substrates (roughness of about 0.1 μm). The first three films were deposited at the optimum oxygen partial pressure of 5×10^{-6} mbar, whereas the fourth film was fabricated at a much higher oxygen partial pressure of 1×10^{-4} mbar. Accordingly, this film consisted of a mixture of Fe_3O_4 and Fe_2O_3 as already evident from its brownish colour. Film thickness was 80 nm (epitaxial film), 120 nm (polycrystalline films on $MgAl_2O_4$) and 150 nm (epitaxial film on sapphire). An X-ray scattering analysis yielded the following information. The magnetite film on epi-polished $MgAl_2O_4$ grew epitaxially; in a Θ-2Θ scan only the [00L] reflexes were detectable. Rocking curves in Θ- and 2Θ-scans were analyzed yielding information about mosaicity and defects along the growth direction, respectively. We found values of full width at half maximum (FWHM) of the rocking curves for the (004) reflection: FWHM(Θ) = 1.06° and FWHM(2Θ) = 0.52°; these are typical for magnetite films grown on $MgAl_2O_4$ and are due to the rather large lattice mismatch of 3.9% (Fe_3O_4: 8.398 Å, $MgAl_2O_4$: 8.0835 Å). The magnetite film on sapphire had polycrystalline character. It grew mainly (111) oriented; in a wide angle $\Theta-2\Theta$ scan, however, both (LLL) and (00L) reflexes were seen. An analysis of the rocking curves of the (222) and (004) reflections yielded the following values: (1) [111]: FWHM(Θ) = 1.0°, FWHM(2Θ) = 0.44° and (2) [001]: FWHM(Θ) = 14°, FWHM(2Θ) = 1.7°. A Θ-Φ scan of the (224) reflex showed a sixfold symmetry; a value of FWHM(Θ) = 1.0° was obtained in agreement with the analysis of the symmetric (222) reflex. The in-plane misalignment was estimated by the full width at half maximum of the Φ scan to 6°. No X-ray signal could be detected for the magnetite films on the rough $MgAl_2O_4$ backside. Since the film thickness was in the same range, this attests to the minor crystallographic quality and the desired polycrystalline character of those films.

A $La_{0.7}Ca_{0.3}MnO_3$ (LCMO) film was grown by pulsed laser deposition on MgO (001) from a stoichiometric, polycrystalline LCMO target. Substrate temperature was 650 °C and oxygen partial pressure 0.13 mbar. In this case an Excimer laser (Lambda-Physik) was used at a wavelength of 308 nm (XeCl) and a pulse energy of 0.2 J; fluence was about 2 J/cm^2. Film thickness was 250 nm.

Magnetotransport measurements were performed within a He flow cryostat system equipped with a 9 T superconducting magnet. The field was applied parallel to the main area of the films. A conventional four-point dc technique using a constant current source (Keithley model 224) and a nanovoltmeter (Keithley model 182) were employed for most of the measurements. This system works reliably up to about 0.5 GΩ. The Fe_3O_4/Fe_2O_3 film had such a high resistance that the measurements had to be performed with a capacitance/loss bridge (Andeen-Hagerling 2500 A) operating at 1 kHz in a two-point configuration. This setup works reliably up to 5000 GΩ. Magnetization measurements were performed with a Quantum Design MPMS-7 SQUID magnetometer.

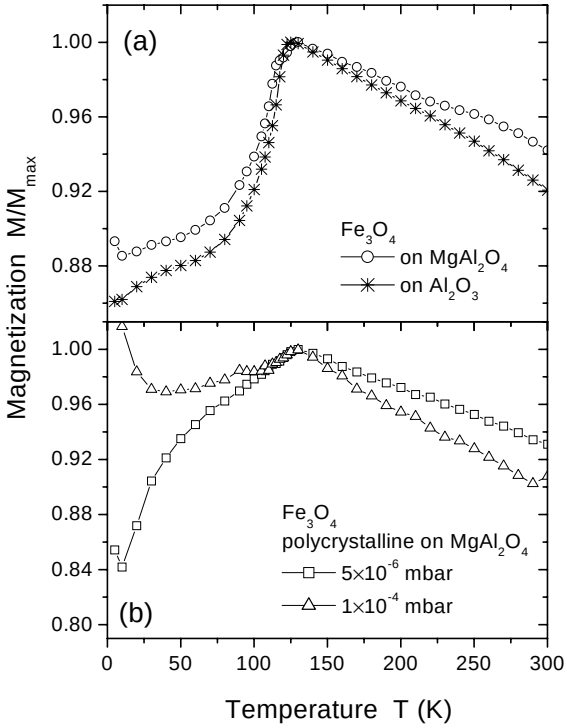

Fig. 1. Magnetization of the Fe_3O_4 films investigated. The magnetization was measured after zero field cooling in an applied magnetic field of 0.2 T. Results for the epitaxial film on $MgAl_2O_4$ and the polycrystalline film on sapphire are shown in (a), the magnetization of the polycrystalline films on $MgAl_2O_4$ are shown in (b).

3 Results

3.1 Magnetization and zero field resistivity

Figure 1 shows the temperature dependent magnetization of the magnetite films studied in this work. The magnetization was measured on warming in a magnetic field of 0.2 T applied at 10 K after zero field cooling. Both the epitaxial film on $MgAl_2O_4$ and the polycrystalline film on Al_2O_3 show a clear Verwey transition; the Verwey temperature as determined from the maximum slope of the magnetization is 115 K. Sena *et al.* [23] investigated the properties of magnetite films on MgO as a function of film thickness and found a Verwey temperature of about 110 K at a film thickness of 100 nm. Taking the film thickness of 80 nm into account this comparison indicates that the

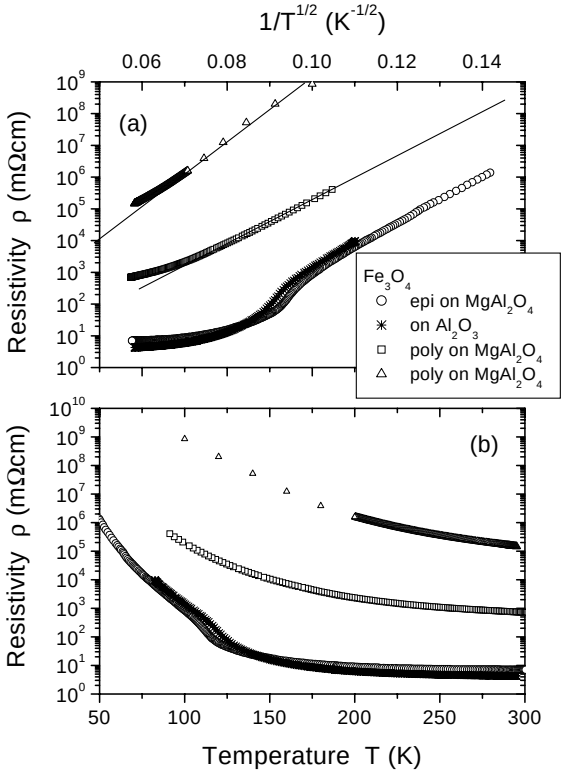

Fig. 2. Resistivity of the Fe_3O_4 films investigated shown in (a) as a function of $T^{-1/2}$ and in (b) as a function of temperature.

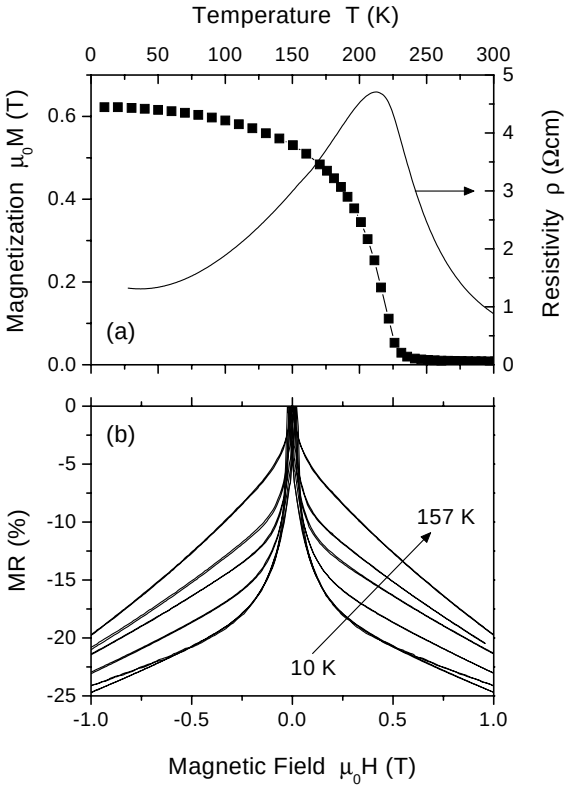

Fig. 3. (a) Magnetization (left axis) and zero field resistivity (right axis) as well as (b) magnetoresistance of the polycrystalline LCMO film on MgO.

epitaxial film is of good quality. There is no jump visible in the magnetization of the polycrystalline films fabricated on rough $MgAl_2O_4$ shown in Figure 1b; the small maximum at 125 K, however, might be a remnant of the Verwey transition; its shallowness, however, precludes the determination of a Verwey temperature.

Figure 2 shows the zero field resistivity as a function of $T^{-1/2}$ (a) and temperature T (b). In case of the epitaxial film on $MgAl_2O_4$ and the film on Al_2O_3 a clear Verwey transition at temperatures of 112 K ($MgAl_2O_4$) and 118 K (Al_2O_3) can be observed consistent with the magnetization data. In case of the polycrystalline films no indication of a Verwey transition could be detected in the resistivity data. Whereas the former two films have room temperature resistivities of 7.7 mΩcm ($MgAl_2O_4$) and 4.3 mΩcm (Al_2O_4) in good agreement with the bulk value of 4 mΩcm [24], the latter show a strong resistivity enhancement. This indicates that the resistivity of these films is dominated by grain-boundary transport processes. Moreover, the high resistivity of the Fe_3O_4/Fe_2O_3 film indicates that haematite might be nucleated near grain boundaries. The resistivity of these polycrystalline films varies as $\exp[(T_0/T)^{1/2}]$ indicating their granular nature [25].

Magnetization and magnetotransport data of the LCMO film on MgO are shown in Figure 3. According to the deposition conditions this film is expected to be polycrystalline and this is borne out by the magnetotransport data [26]. The Curie temperature determined from the steepest slope of the magnetization is 219 K. The zero field resistivity is large compared to values of epitaxial films [27]. The important characteristic is, however, that the magnetoresistance increases monotonically with decreasing temperature proving its extrinsic nature [2,3]. There is a bulk of evidence that the low-field magnetoresistance in polycrystalline LCMO samples is due to spin-polarized tunnelling [1]. Therefore we regard this film as a prototype system for further comparison with the magnetite films.

3.2 Magnetoresistance: Fe_3O_4 on $MgAl_2O_4$ and Al_2O_3

In the following magnetoresistance data will be discussed; the magnetoresistance definition

$$MR = \frac{\rho(H,T) - \rho(0,T)}{\rho(0,T)} \tag{1}$$

will be used throughout. The magnetoresistance of the epitaxial magnetite film on $MgAl_2O_4$ and the film on sapphire are compared in Figure 4 in the temperature range between 60 K and 220 K and for magnetic fields up to 6 T. The most important difference between both data-sets is the strong magnetoresistance enhancement seen for the film on sapphire. The magnetoresistance of this film increases with decreasing temperature showing that this is

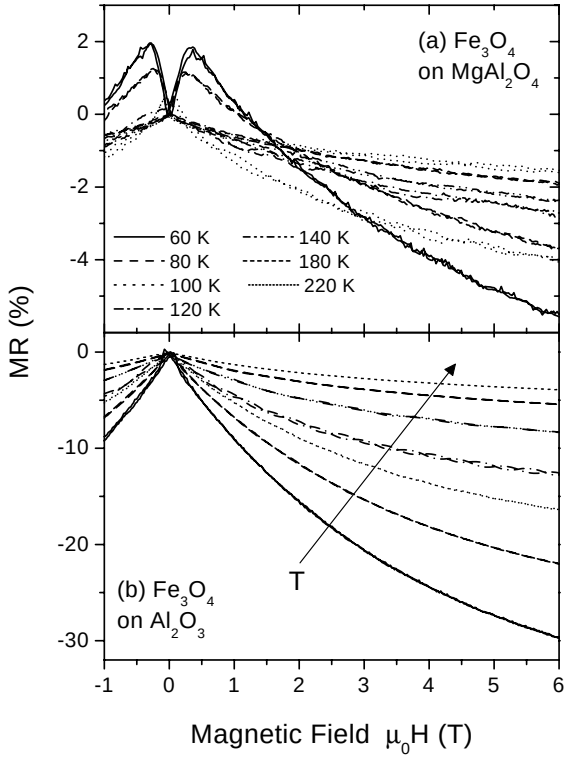

Fig. 4. Magnetoresistance of the Fe_3O_4 films on (a) $MgAl_2O_4$ and (b) sapphire at various temperatures.

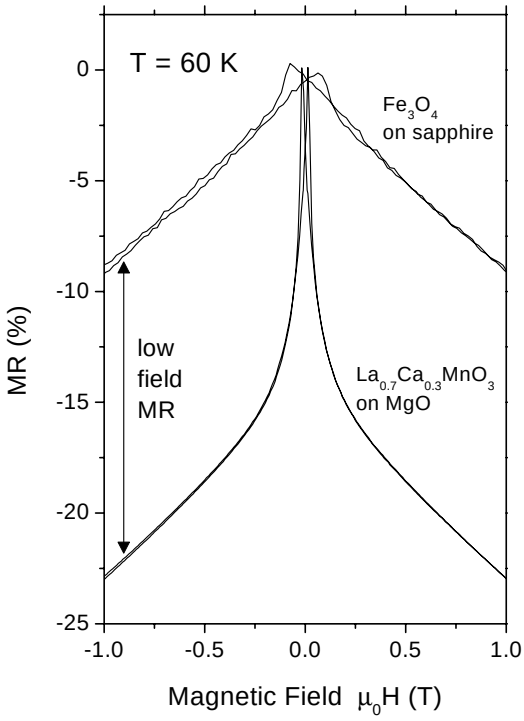

Fig. 5. Comparison of the magnetoresistance of the polycrystalline Fe_3O_4 film on sapphire and a polycrystalline $La_{0.7}Ca_{0.3}MnO_3$ film on MgO.

an extrinsic effect. Since this film is polycrystalline, it seems reasonable to attribute this enhancement to grain-boundary scattering. The non-monotonic field dependence of the magnetoresistance of the epitaxial film is due to anisotropic magnetoresistance [22]. In order to elucidate the mechanism for the extrinsic magnetoresistance, in Figure 5 we compare the data obtained for the magnetite film on sapphire at 60 K with the magnetoresistance of the polycrystalline LCMO film at the same temperature. This comparison is striking: the large low-field resistance drop that is the signature of spin-polarized tunnelling in polycrystalline LCMO films is absent in the polycrystalline magnetite film, whereas the high-field magnetoresistance slopes are similar. This indicates that the magnetoresistance enhancement observed in the Fe_3O_4 film on sapphire in comparison to the epitaxial Fe_3O_4 film is caused by the same processes that produce the high-field magnetoresistance slope ubiquitously seen in polycrystalline manganite films.

For a further analysis we compared the magnetoresistance to the square of the measured magnetization. In case of spin-polarized tunnelling the tunnelling conductance between adjacent grains is proportional to $\cos(\Theta)$, where Θ denotes the relative angle between the grain magnetizations. Averaging over grains yields a magnetoresistance proportional to $\langle\cos(\Theta)\rangle = (M/M_S)^2$. M_S denotes the saturation magnetization. In Figure 6a the low-field magnetoresistance of the polycrystalline LCMO film at 100 K is shown. A clear scaling

$$MR = C(M/M_S)^2 \qquad (2)$$

with $C = 0.14$ is observed. At high magnetic fields M saturates and as shown in Figure 6 the scaling breaks down above 0.1 T, where the steep low-field magnetoresistance crosses over into the high-field magnetoresistance linear in field. This high-field magnetoresistance is due to the polarization of the grain-boundary magnetization that is not detectable in the global magnetization, since the grain-boundary fraction is too small. The coefficient C defined in equation (2) is shown in Figure 7 as a function of temperature. At low temperatures < 150 K it follows a M_S^4 law.

In case of the Fe_3O_4 film on Al_2O_3 the situation is different. Figure 8 clearly shows that it is difficult to obtain a scaling between the magnetoresistance and $(M/M_S)^2$ at low fields; moreover, the $(M/M_S)^2$-dependence accounts only for 1–2% of the magnetoresistance. From Figure 8 it is evident that the major part of the magnetoresistance in this polycrystalline magnetite film does not scale with the square of the magnetization. Therefore, we attribute this part to spin-disorder scattering at the grain-boundaries [1,28–30]. We conclude from these measurements that spin-polarized tunnelling between misaligned grains as seen in polycrystalline manganites is absent in most polycrystalline magnetite films, compare also the data in [9–16]. The high-field magnetoresistance due to spin-dependent scattering within the grain boundary is similar to the case of epitaxial Fe_3O_4 films on MgO showing a high-field magnetoresistance attributed to scattering at antiphase boundaries [31].

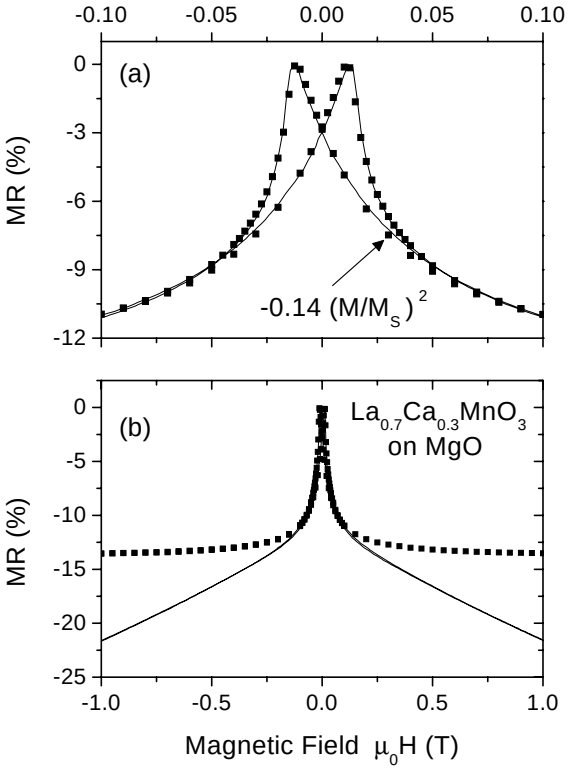

Fig. 6. Magnetoresistance ratio of the $La_{0.7}Ca_{0.3}MnO_3$ film on MgO at 100 K (solid lines) compared to the square of the magnetization (symbols) measured in magnetic fields (a) up to 0.1 T and (b) up to 1 T.

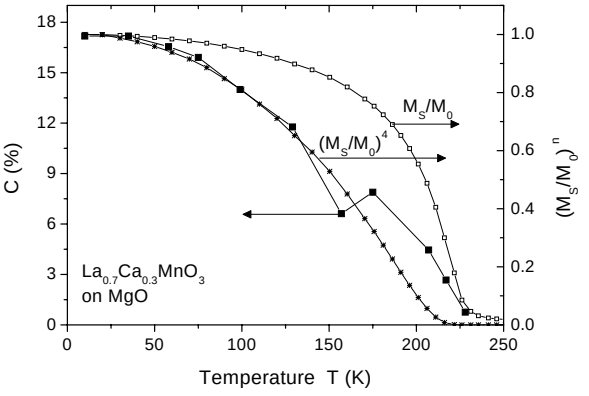

Fig. 7. In the case of polycrystalline $La_{0.7}Ca_{0.3}MnO_3$ the low-field magnetoresistance follows $MR = -C(M/M_S)^2$. The experimentally determined coefficient C is shown here in comparison to the reduced saturation magnetization M_S/M_0 and $(M_S/M_0)^4$. M_0 denotes the saturation magnetization at zero temperature.

3.3 Magnetoresistance: Fe_3O_4 on rough $MgAl_2O_4$

The absence of a low-field magnetoresistance in polycrystalline films on sapphire might be related to (1) a vanishing spin-polarization, (2) conducting grain-boundaries not forming tunnelling barriers or (3) a strong magnetic coupling between grains preventing an independent switching of these. Since the magnetite film on sapphire is stoichiometric as judged from the Verwey transition seen in both resistivity and magnetization, explanation (1) seems unrealistic. In order to study alternatives (2) and (3) we measured the magnetotransport properties of the polycrystalline films on rough $MgAl_2O_3$ substrates. Since these show a strong enhancement of the resistivity, the grain boundaries are likely to act as tunnel barriers in these films. The magnetoresistance in the temperature range between 80 K and 200 K is shown in Figure 9 in steps of 20 K. The magnetoresistance decreases monotonically with temperature in agreement with its extrinsic nature. The magnitude of the magnetoresistance, however, is small, considerably smaller than in the case of the polycrystalline film on sapphire. Moreover, the magnetoresistance is independent of the Fe_2O_3 content.

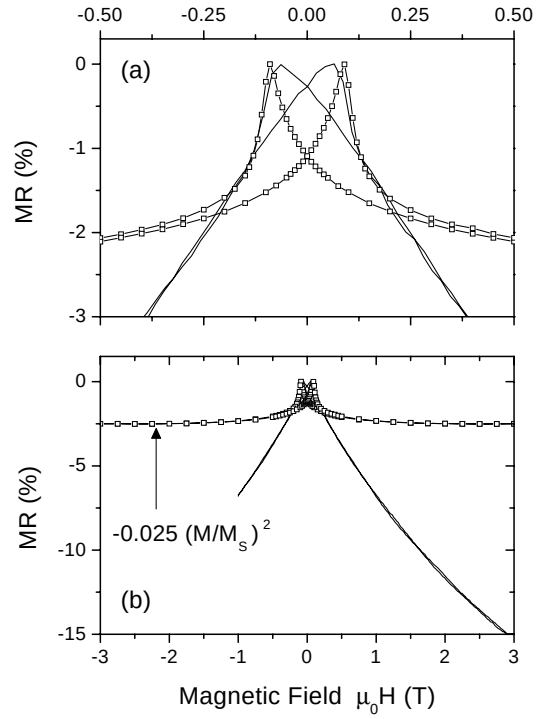

Fig. 8. Magnetoresistance ratio of the Fe_3O_4 film on sapphire at 80 K compared to the square of the measured magnetization on field scales of (a) 0.5 T and (b) 3 T.

The polycrystalline films on rough $MgAl_2O_4$ behave as granular metals. This is indicated by the zero field resistivity following a $\exp[(T_0/T)^{1/2}]$ law. Below 140 K the magnetoresistance is independent of temperature. This might indicate a tunnelling mechanism, since the magnetoresistance in granular ferromagnets is given by [33]

$$MR = \frac{P^2}{1+P^2} \tag{3}$$

and the spin-polarization P should be independent of temperature far below the Curie temperature. On the other hand, a scaling of the magnetoresistance with $(M/M_S)^2$ according to equation (2) can only be found with $C \sim 0.01$ as is the case for the magnetite film on sapphire. Following this criterion, the magnetoresistance in these

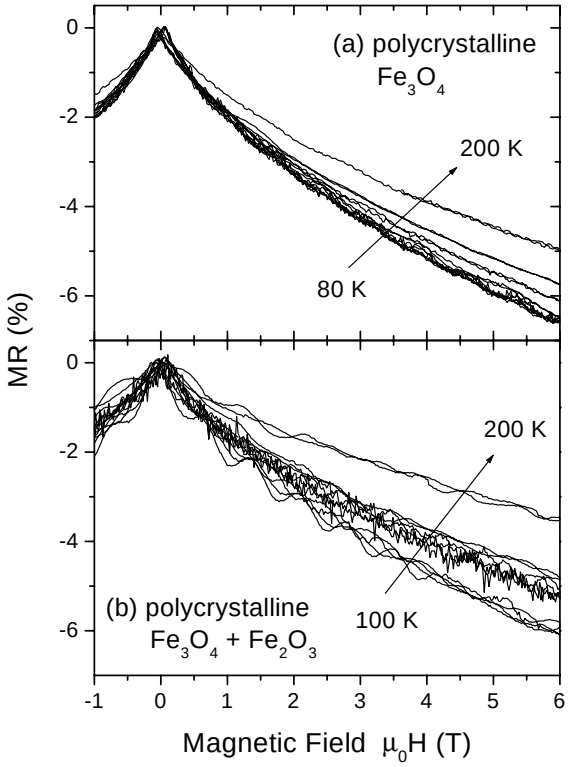

Fig. 9. Magnetoresistance of the polycystalline Fe_3O_4 films on $MgAl_2O_4$ at various temperatures.

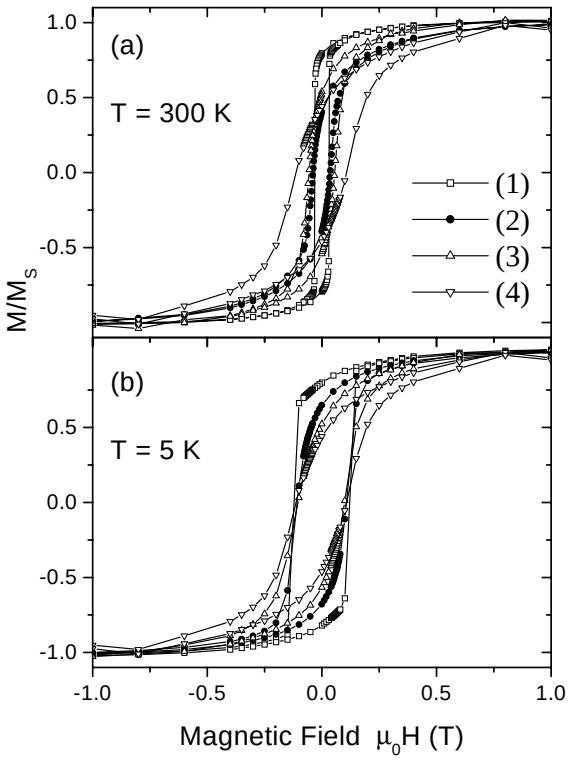

Fig. 10. Magnetization hysteresis loops at (a) 300 K and (b) 5 K of the films investigated in this work: (1) epitaxial Fe_3O_4 on $MgAl_2O_4$, (2) magnetite on sapphire, (3) Fe_3O_4 on rough $MgAl_2O_4$ and (4) Fe_3O_4/Fe_2O_3 on rough $MgAl_2O_4$.

disordered films is mainly due to spin-dependent scattering at grain-boundaries.

The absolute magnitude of the magnetoresistance in these films is considerably smaller than for the film on sapphire. This might be related to a decrease of the spin-polarization due to non-stoichiometry near the grain boundaries. This is supported by the absence of a clear Verwey transition in both magnetization and resistivity.

The magnetic coupling between grains is reflected in the squareness of the hysteresis loops. In Figure 10 magnetization hysteresis loops of the four films at (a) 300 K and (b) 5 K are compared. It can be clearly seen that the switching field distribution systematically broadens with the epitaxial film having the sharpest and the Fe_3O_4/Fe_2O_3 film on rough $MgAl_2O_4$ having the widest distribution. This corresponds well to the degree of granularity as inferred from X-ray scattering and resistivity. These data indicate that there is a gradual magnetic decoupling of grains as structural quality becomes worse.

3.4 Modelling the magnetoresistance

The magnetoresistance arising at anti-phase boundaries in epitaxial magnetite films on MgO was analyzed by Ziese and Blythe [31] and Eerenstein *et al.* [32] within one-dimensional models. Here the grain-boundary magnetoresistance will be analyzed along similar lines. Since electron hopping occurs on B-sites, considerations will be restricted to the ferromagnetically coupled B-site sublattice. The grain boundary is supposed to consist of a layer of n spins with local spin orientations being tilted at random by an average angle Θ_0 with respect to the spins within the grains. This is indicated in Figure 11a. A local exchange field $\mathbf{B}_{ex}$ is introduced to model this tilt as shown in Figure 11b. The application of an external induction $\mathbf{B}$ leads to a rotation of the magnetic moment $\boldsymbol{\mu}$. The rotation angle Θ is given by minimization of the energy

$$E = -\mu \left[B\cos(\Theta) + B_{ex}\cos(\Theta - \Theta_0)\right] \qquad (4)$$

with the solution $B/B_{ex} = \sin(\Theta_0 - \Theta)/\sin(\Theta)$. The hopping matrix element for hopping between B-sites is reduced by the factor $\cos(\Theta/2)$ from the spin rotation. Thus the conductivity across the grain boundary can be written within a one-dimensional model as $\sigma \propto \cos^{(n+1)}(\Theta)$ such that the magnetoconductance is given by

$$\frac{\Delta\sigma}{\sigma} = \frac{\sigma(B) - \sigma(0)}{\sigma(0)} = \frac{\cos^{n+1}(\Theta) - \cos^{n+1}(\Theta_0)}{\cos^{n+1}(\Theta_0)}\,. \qquad (5)$$

Figure 12a shows the magnetoconductance measured for the magnetite film on sapphire at 60 K. Assuming $n = 10$, a satisfactory modelling of the experimental data can be obtained with a tilt angle $\Theta_0 = 40°$ and a local exchange field $B_{ex} = 13$ T. As shown in Figure 12b the magnetoconductance data are strongly temperature

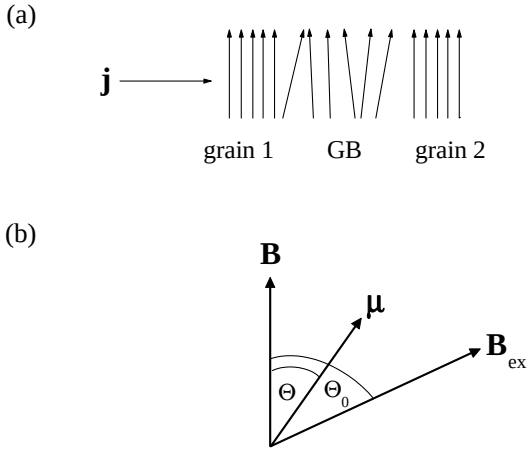

Fig. 11. (a) Schematic drawing of a disordered grain-boundary region with grains to the left and right. For simplicity only B-site spins are shown. (b) Applied field **B**, local exchange field $\mathbf{B}_{ex}$ and magnetic moment $\boldsymbol{\mu}$ of a grain-boundary spin rotated by an angle Θ towards the applied field from its initial position parallel to the local exchange field.

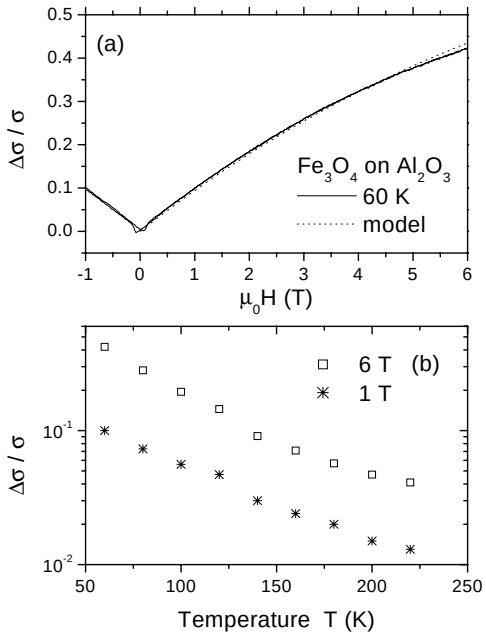

Fig. 12. (a) Magnetoconductance $\Delta\sigma/\sigma = [\sigma(H) - \sigma(0)]/\sigma(0)$ of the magnetite film on sapphire at 60 K. The dotted line is a simulation of the magnetoconductance within the one-dimensional grain-boundary scattering model. (b) Temperature dependence of the magnetoconductance measured at 1 T and 6 T for the Fe_3O_4 film on sapphire.

dependent, whereas the model calculation is temperature independent. The calculations of Ziese and Blythe [31] for the magnetoresistance across antiphase boundaries yielded some temperature dependence in agreement with the data for epitaxial films, but too small to explain the almost exponential decay of the magnetoconductance observed here. This exponential behaviour is reminiscent of a Debye-Waller factor and might be related to strong thermally excited angular rotations due to interfacial spin waves. The development of an elaborate model taking into account a more realistic grain-bounday structure and spin-wave excitations would be helpful for a better understanding of the data.

4 Conclusions

In this work the magnetic and magnetotransport properties of magnetite films with different microstructure have been investigated and compared to results for a typical polycrystalline LCMO film. Aim of this study was the identification of prerequisites to observe spin-polarized tunnelling in polycrystalline magnetite. We used a criterion based on a scaling between magnetoresistance and the square of the magnetization as an indicator for tunnelling transport (although this indicator is not unique). Although polycrystalline magnetite films can have a large magnetoresistance in high fields, the typical low-field magnetoresistance due to spin-polarized tunnelling between individual grains is virtually absent. The high-field magnetoresistance arises from spin-dependent scattering at the spin-disordered interfaces.

In the interpretation of these data two competing effects have to be taken into account. On the one hand the introduction of grain boundaries leads to an enhancement of the magnetoresistance, but not of the resistivity; this is the case in a polycrystalline film on sapphire: here the grain boundaries do not act as tunnelling barriers and a magnetotunnelling mechanism cannot be expected. On the other hand, magnetite films prepared on rough $MgAl_2O_4$ films show a considerable resistivity enhancement; in these films, however, the Verwey transition is not observed any more indicating a significant non-stoichiometry which – in turn – implies a reduced spin-polarization. The evaluation of magnetization hysteresis loops indicates a broad switching field distribution in polycrystalline films; we interpret this as indicating decoupled grains. Since magnetite is a bad metal with a resistivity above the Ioffe-Regel limit [34], one might speculate if such a system can show tunnelling transport at all.

This work was supported by the DFG under Contract No. DFG ES 86/7-1 within the Forschergruppe "Oxidische Grenzflächen".

References

1. M. Ziese, Rep. Prog. Phys. **65**, 143 (2002)
2. H.Y. Hwang, S.W. Cheong, N.P. Ong, B. Batlogg, Phys. Rev. Lett. **77**, 2041 (1996)
3. A. Gupta, G.Q. Gong, G. Xiao, P.R. Duncombe, P. Lecoeur, P. Trouilloud, Y.Y. Wang, V.P. Dravid, J.Z. Sun, Phys. Rev. B **54**, R15629 (1996)
4. H.Y. Hwang, S.-W. Cheong, Science **278**, 1607 (1997)

5. H.Y. Hwang, S.-W. Cheong, Nature (London) **389**, 942 (1997)
6. T.H. Kim, M. Uehara, S.-W. Cheong, S. Lee, Appl. Phys. Lett. **74**, 1737 (1999)
7. A. Yanase A, N. Hamada, J. Phys. Soc. Jpn **68**, 1607 (1999)
8. C. Srinitiwarawong, G. Gehring, J. Phys. Cond. Matt. **13**, 7987 (2001)
9. J.M.D. Coey, A.E. Berkowitz, Ll. Balcells, F.F. Putris, F.T. Parker, Appl. Phys. Lett. **72**, 734 (1998)
10. M. Ziese, C. Srinitiwarawong, C. Shearwood, J. Phys. Cond. Matt. **10**, L659 (1998)
11. J.S.-Y. Feng, R.D. Pashley, M.-A. Nicolet, J. Phys. C **8**, 1010 (1975)
12. X.W. Li, A. Gupta, G. Xiao, G.Q. Gong, J. Appl. Phys. **83**, 7049 (1998)
13. K. Nishimura, Y. Kohara, Y. Kitamoto, M. Abe, J. Appl. Phys. **87**, 7127 (2000)
14. Y. Kitamoto, Y. Nakayama, M. Abe, J. Appl. Phys. **87**, 7130 (2000)
15. M. Uotani, T. Taniyama, Y. Yamazaki, J. Appl. Phys. **87**, 5585 (2000)
16. T. Taniyama, Y. Kitamoto, Y. Yamazaki, J. Appl. Phys. **89**, 7693 (2001)
17. X.W. Li, A. Gupta, G. Xiao, W. Qian, V.P. Dravid, Appl. Phys. Lett. **73**, 3282 (1998)
18. P.J. van der Zaag, P.J.H. Bloemen, J.M. Gaines, R.M. Wolf, P.A.A. van der Heijden, R.J.M. van der Veerdonk, W.J.M. de Jonge, J. Magn. Magn. Mater. **211**, 301 (2000)
19. J.J. Versluijs, J.M.D. Coey, J. Magn. Magn. Mater. **226-230**, 688 (2001)
20. J.J. Versluijs, M.A. Bari, J.M.D. Coey, Phys. Rev. Lett. **87**, 026601 (2001)
21. P. Chen, D.Y. Xing, Y.W. Du, J.M. Zhu, D. Feng, Phys. Rev. Lett. **87**, 107202 (2001)
22. R. Höhne, M. Ziese, N.H. Hong, H.-C. Semmelhack, P. Esquinazi, unpublished
23. S.P. Sena, R.A. Lindley, H.J. Blythe, Ch. Sauer, M. Al-Kafarji, G.A. Gehring, J. Magn. Magn. Mater. **176**, 111 (1997)
24. P.A. Miles, W.B. Westphal, A. von Hippel, Rev. Mod. Phys. **29**, 279 (1957)
25. P. Sheng, B. Abeles, Y. Arie, Phys. Rev. Lett. **31**, 44 (1973)
26. I. Satoh, T. Kobayashi, Jpn J. Appl. Phys. **40**, 586 (2001)
27. M. Ziese, S.P. Sena, J. Phys. Cond. Matt. **10**, 2727 (1998)
28. M. Ziese, Phys. Rev. B **60**, R738 (1999)
29. J.E. Evetts, M.G. Blamire, N.D. Mathur, S.P. Issac, B.-S. Teo, L.F. Cohen, J.L. MacManus-Driscoll, Phil. Trans. R. Soc. London A **356**, 1593 (1998)
30. P. Guinea, Phys. Rev. B **58**, 9212 (1998)
31. M. Ziese, H.J. Blythe, J. Phys. Cond. Matt. **12**, 13 (2000)
32. W. Eerenstein, T.T.M. Palstra, S.S. Saxena, T. Hibma, Phys. Rev. Lett. **88**, 247204 (2002)
33. I. Inoue, S. Maekawa, Phys. Rev. B **53**, R11927 (1996)
34. *Spin Electronics*, edited by M. Ziese, M.J. Thornton (Springer Verlag, Heidelberg, 2001)